Algal Research 83 (2024) 103732



Contents lists available at ScienceDirect

Algal Research

journal homepage: www.elsevier.com/locate/algal





Improved hydrogen production in immobilized *Chlamydomonas reinhardtii* cells with inhibited inter-photosystem electron transfer

Fatemeh Khosravitabar [a,b], Fikret Mamedov [a,*]

[a] Molecular Biomimetics, Department of Chemistry – Ångström Laboratory, Uppsala University, Box 523, 75120 Uppsala, Sweden
[b] Department of Biological and Environmental Sciences, University of Gothenburg, 40530 Gothenburg, Sweden

ARTICLE INFO

Keywords:
H_2 production
Chlamydomonas reinhardtii
Immobilization
Alginate beads
DBMIB

ABSTRACT

The production of molecular hydrogen (H_2) by microalgae holds great promise, and immobilization techniques offer potential for further advancement in this field. The current study focuses on investigating the positive impact of immobilization on maintaining the stability and activity of photosystem II (PSII) over incubation time, with the aim of enhancing H_2 production potential in green microalgae *Chlamydomonas reinhardtii*. For this purpose, immobilized cells within alginate beads were treated with small concentrations of 2,5-dibromo-3-methyl-6-isopropyl-p-benzoquinone (DBMIB) inhibitor to induce the partial inhibition of inter-photosystem electron transport, recently reported as a novel approach for sustaining microalgal H_2 production. A comparative analysis of fluorescence decay kinetic changes and EPR spectroscopy of the cell beads revealed the superior capacity of immobilization for sustaining PSII stability and activity in batch culture over time. Treatment of the cell beads with 3.5 μM DBMIB led to sustained H_2 production yielding over 200 μmol H_2/mg Chl within 3 weeks, with an average H_2 production rate of approximately 10 μmol/mg Chl per day, both of which were roughly twice as high as those observed in free cells treated with DBMIB. Our findings underscore the significance of integrating immobilization with a proven and effective method for H_2 production, thereby enhancing its sustainability and productivity.

1. Introduction

Cell immobilization presents several advantages for enhancing the sustainability of microalgal cultivation [1,2]. These advantages become more important for the transition of various microalgal cultures from the laboratory to large scale applications [3,4]. Firstly, immobilization separates cells from the liquid phase, facilitating cell harvesting and reducing associated costs [5,6]. Secondly, it physically confines microalgae to support materials, effectively mitigating the risk of contamination from other microorganisms [7]. Thirdly, when compared to free cells, immobilized microalgae have demonstrated increased resistance against various environmental stress factors, leading to improved cell viability [7–9]. Eventually, immobilization allows for the accumulation of higher cell densities and, therefore, increased productivity [7–9]. One promising, although not yet commercially mature, application of green microalgal cultivation is molecular hydrogen (H_2) production [6,10–14], and leveraging immobilization could advance this application towards commercial viability.

H_2 serves as a unique energy carrier which can be produced by certain green microalgal species through two distinct metabolic pathways directly or indirectly linked to the photosynthetic process. The direct pathway relies on the electron transfer initiated by water splitting in PSII through the cytochrome (Cyt) b_6f complex and PSI to the hydrogenase enzyme (HydA in Chlamydomonas), catalyzing the conversion of electrons and protons to molecular H_2. The indirect pathway utilizes carbohydrate degradation to transfer electrons via the plastoquinone (PQ) pool through the Cyt b_6f complex and PSI to HydA [15]. However, in nature, H_2 production via both pathways is only transient (a few minutes) due to the extreme sensitivity of HydA to molecular oxygen (O_2), which is produced by PSII during illumination [16]. Efforts have been made to extend and enhance H_2 photoproduction. Initially, studies in this area focused on inhibiting or down-regulating the PSII activity through a mutagenetic approach [17–19] or nutrient deficiency [20–23], mostly resulting in several days of H_2 production. This two-stage medium-term H_2 production in Chlamydomonas requires a certain level of reduction of the PQ pool and anoxia in the chloroplast, usually achieved after the first stage [24].

It was demonstrated that achieving this reduction could be done by

* Corresponding author.
E-mail addresses: fatemeh.khosravitabar@bioenv.gu.se (F. Khosravitabar), fikret.mamedov@kemi.uu.se (F. Mamedov).

https://doi.org/10.1016/j.algal.2024.103732
Received 26 April 2024; Received in revised form 14 July 2024; Accepted 28 September 2024
Available online 2 October 2024
2211-9264/© 2024 The Authors. Published by Elsevier B.V. This is an open access article under the CC BY license (http://creativecommons.org/licenses/by/4.0/).

directly regulating photosynthetic electron transfer reactions outside of the PSII domain without nutrient limitations. This includes decreasing the amount of PSI or partially inhibiting the Cyt b_6f complex [25,26]. Supporting this, mutants with impaired cyclic electron flow, like *pgr5* and *hpm91* mutants [27,28], also resulted in the increased H_2 production as well as creating anoxia by using O_2-scavengers [29,30].

It is well-established that PSII plays a pivotal role in the long-term H_2 photoproduction [24,31,32]. Therefore, greater stability of PSII, and photosynthetic reactions in general, can potentially promote H_2 production in green microalga. Previous studies have already utilized immobilized microalgae or cyanobacteria for H_2 production [33–36]. In Chlamydomonas, combining immobilization with the two-phase sulfur-deficiency method demonstrated higher specific rates [37], prolonged [38] and more efficient [39] H_2 production when compared to only free cells under sulfur-deprivation.

We hypothesized that since the immobilization technique enhances the cell viability, it could also promote the stability of PSII. Thus, combining immobilization with other more direct, single staged methods for H_2 production could potentially result in a more robust and enduring H_2 output. We relied on our recently published approach [26], when the redox state of the PQ-pool was regulated with a small amount of the 2,5-dibromo-3-methyl-6-isopropyl-p-benzoquinone (DBMIB) inhibitor acting on the Cyt b_6f complex. By adopting this method, we achieved H_2 production in a liquid culture of wild type Chlamydomonas that extended for up to 4 weeks and resulting in accumulative output of around 100 μmole H_2/mg Chl. This outcome was achieved when the culture (initially containing approximately 8 million cells per ml of TAP medium), was treated with a suboptimal concentration of 3.5 μm DBMIB. This preceding study showed that a controlled increase in the reduction level of the PQ-pool not only slows down the inter-photosystem electron transport but also stimulates the O_2 photorespiration processes, ultimately leading to a high level of H_2 production while maintaining substantial PSII activity [26]. Our innovative approach in the current manuscript integrates immobilization and inter-photosystem electron transport regulation. We aim to optimize conditions and harness the synergistic benefits of both techniques to further enhance H_2 production.

2. Materials and methods

2.1. Growth conditions and cell immobilization

Chlamydomonas reinhardtii wild-type CC-5325 strain was grown in liquid TAP medium at 25 °C under constant illumination at an intensity of 60 μE × m^{-2} s^{-1} and shaking at 120 rpm. Mid-log phase cells (at 10 μg Chl/ml or 4 × 10^6 cells/ml) were collected by centrifugation at 2000 × *g* for 3 min, and then resuspended in fresh TAP medium to form a concentrated algal suspension at approximately 77 μg Chl/ml. Subsequently, the immobilization of cells in alginate beads was executed following the approach outlined in [40], with some modifications. Essentially, the concentrated algal suspension was blended with a 4.5 % sodium alginate solution, maintaining a 1:1 volume ratio. This resultant mixture was introduced into a 100 ml burette and, upon release, drops were formed as they were gently introduced into a $CaCl_2$ solution (2 %) as a cross-linking agent. This method yielded consistently sized algal beads, roughly 2.5 mm in diameter, each containing an initial cell count of 1.2 million cells per bead (equivalent to 5 μg Chl). The freshly formed beads underwent constant mixing in the $CaCl_2$ solution for 3 h at room temperature to ensure their proper hardening. Afterward, the beads were thoroughly rinsed with sterile distilled water and then transferred to either T75 culture flasks for characterization or 20 ml gas-tight vials for the H_2 production experiments.

For cell density estimation, 10 randomly selected beads were dissolved in 5 ml of 0.5 M tri-sodium citrate solution with 10 min of mixing. Cell counting was performed using a hemocytometer and recorded as cell numbers per bead or as μg Chl per bead to be employed in further calculations [41].

2.2. Characterization of microalgae beads during long-term incubation

Freshly created beads were placed in T75 flasks, each with 200 beads and 40 ml fresh TAP medium (Fig. 1A). The formed beads were incubated under continuous illumination at 60 μE m^{-2} s^{-1} at 25 °C for 30 days, with one medium replenishment after 2 weeks. At various intervals (1, 2, 4, 10, 20, and 30 days), 10 random bead samples were taken to be directly used in flash-induced variable fluorescence measurements. This assessment was performed as was described before [24,25,42]. In each instance, 10 beads, along with 500 μl of TAP medium, were placed in a cuvette and incubated in the dark for 2 min before the measurement. A suspension culture, at concentration of 77 μg Chl/ml, served as a control. Where indicated, 20 μl DCMU was added to the bead media before the measurement. It should be mentioned, that no bead breakage or cell leakage has been observed during the course of our experiments.

Electron paramagnetic resonance (EPR) measurements to quantify PSII and PSI amounts were performed with Bruker BioSpin EMX-micro spectrometer equipped with EMX-Premium bridge according to the previously established method [25,26,43]. In contrast to the fluorescence analysis, for EPR measurement, beads were dissolved in tri-sodium citrate solution, followed by centrifugation (2000 ×*g*, 3 min) to concentrate cells for measurements using flat cell.

2.3. H_2 production by DBMIB-treated microalgal beads

To evaluate H_2 production potential of the microalgae beads, fresh beads were placed in 20 ml gas-tight vials (85 beads per each) with 10 ml TAP and 5 ml headspace. The TAP media was supplemented with DBMIB at final concentrations of 3.5 to 10 μM (normalized to initial cell density in suspension culture per each vial). The sealed vials were then incubated under growth conditions for 20 days. Daily quantification of the H_2 levels in the headspace of the vials was carried out by gas chromatography as described previously [25]. Random bead samples from vials (with 3.5 μM DBMIB) were used for fluorescence assessment and EPR measurements. All assessments, such as fluorescence measurements, were conducted either directly, or as for EPR measurement, samples were prepared and sealed in a home-build glovebox to retain anaerobic conditions.

3. Results

3.1. Analysis of PSII electron transport activity in intact Chlamydomonas beads

Flash-induced fluorescence decay measurement is an informative method for analyzing PSII electron transport reactions and H_2 photoproduction in Chlamydomonas cells [42]. We employed this technique to examine PSII electron transport properties in freshly created beads (Fig. 1A) in comparson to free Chlamydomonas cells. In free Chlamydomonas cells, the fluorescence kinetics predominantly indicated rapid forward electron transfer from Q_A^-, constituting over 85 % of the decay (Fig. 1B, black trace). Analysis of the freshly formed alginate beads containing Chlamydomonas cells yielded a trace that closely resembled that of the free cells (Fig. 1B, blue trace), demonstrating the absence of any alterations in the kinetics of PSII electron transport, attributable to bead formation or alginate matrix. Thus, flash-induced fluorescence decay measurement emerges as a reliable approach to monitor PSII activity within the algae-alginate beads.

Moreover, when the beads were exposed to TAP medium containing 20 μM DCMU for 2 min before measurement, full inhibition of the forward electron transfer was observed, leading to a much slower fluorescence decay (Fig. 1B, red trace), similar to the effect of DCMU addition to free cells (not shown). It shows that inhibitor has been

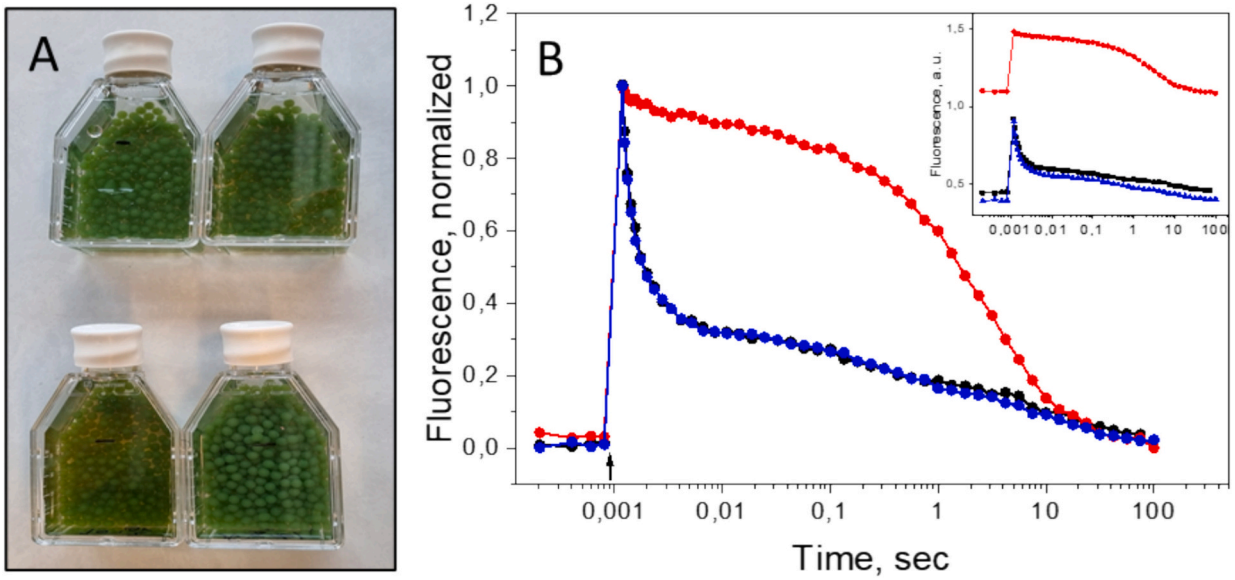


Fig. 1. A. Alginate-encapsulated immobilized cells of *C. reinhardtii* (Chlamydomonas beads) incubated in TAP medium for the long-term storage. B. Flash-induced variable fluorescence decay traces originating from newly formed Chlamydomonas beads in the absence (blue trace) or in the presence of 20 μM DCMU (red trace), in comparison to the trace from fresh free cells of C. reinhardtii (black trace). The arrow marks the flash application time and the inset shows the non-normalized traces. Each trace is the average of measurements from three independent samples. (For interpretation of the references to colour in this figure legend, the reader is referred to the web version of this article.)

effectively absorbed by immobilized cells through the alginate matrix. This suggests that the DBMIB inhibitor could also be absorbed by the entrapped cells in alginate, allowing initiation of H_2 production. This finding supports the rationale for integrating these two approaches in further experiments.

3.2. Stability of photosynthetic electron transport in microalgae beads in the long-term batch culture

To explore the potential benefits of cell immobilization in sustaining photosynthetic activity we measured the flash-induced fluorescence decay kinetics in both free and immobilized cells during a long-term incubation in a batch culture under standard growth conditions. During these measurements, samples were collected and analyzed at various time intervals. Notably, we refrained from normalizing the samples' Chl content across measurements deliberately, aiming to directly compare the sustainability of Chlamydomonas beads versus free cell in a batch culture.

At the onset of incubation, the fluorescence decay kinetics as well as the minimal and maximal fluorescence levels were relatively comparable between concentrated suspension of the free cells (Fig. 2A) and beads (Fig. 2B), black traces, with F_0 and F_M at around 0.4 and 0.9, respectively. These values represent the control fluorescence characteristics of the cells obtained after single saturating flash. After 4 days in the batch culture, free cells exhibited a partial increase in the level of F_0 and a significant reduction of F_M (Fig. 2A, green trace), resulting in a notable drop in the F_V/F_M ratio from 0.53 (day 0) to 0.36 (day 4), as indicated in Table 1. However, there was no significant change in the decay kinetics (Fig. 2A inset, green trace). After 10 days of incubation, free cells displayed a more substantial decline in both F_0 and F_M levels, causing the F_V/F_M ratio to drop to 0.17 (Table 1) and the decay kinetics was slower (Fig. 2A, purple trace) indicating a more reduced state of the acceptor

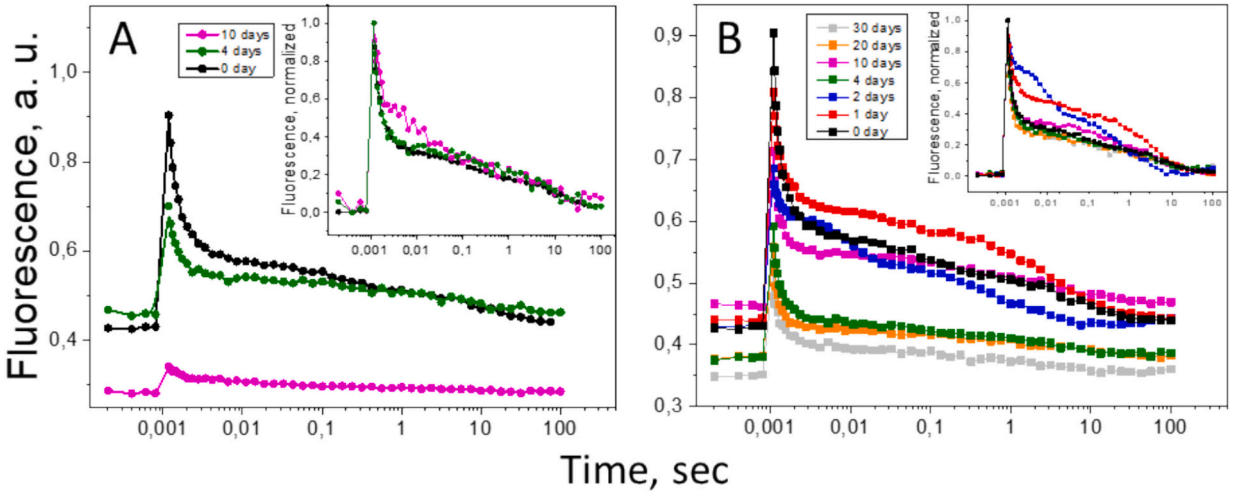


Fig. 2. Changes in the flash-induced fluorescence decay kinetics during the long-term incubation of Chlamydomonas free cells (A) and cell beads (B) in a batch culture. The arrow marks the flash application time and the insets show related normalized traces. Each trace is the average of measurements from three independent samples.

Table 1
Changes in the quantum yield of PSII (F_V/F_M ratio) and PSI/PSII ratio (determined by EPR spectroscopy) in the different Chlamydomonas cultures during the long-term incubation. The results represent the average of three independent measurements.

Time after onset of incubation (days)	Fv/Fm of free cells in TAP	Fv/Fm of cell beads in TAP	Fv/Fm of cell beads in TAP+ 3.5 μM DBMIB	PSI/PSII ratio of cell beads in TAP + 3,5 μM DBMIB
0	0.53	0.52	0.53	0.97
1		0.46	0.21	
2		0.38		
4	0.36	0.35		
10	0.17	0.35	0.41	2.10
20		0.32	0.04	
30		0.32		

side of PSII.

In contrast, cells immobilized within alginate beads responded differently during the long-term incubation period and observable variations in fluorescence decay kinetics for Chlamydomonas beads were notably more pronounced than those for free cells. Initially, during the first 2 days of incubation, the decay kinetics become slower, indicating alteration in the Q_A^- to Q_B electron transfer and Q_B binding (Fig. 2B, red and blue traces). These changes were accompanied with drop in the F_V/F_M ratio from 0.52 to 0.38 (Table 1). However, starting from the day 4 of incubation, as shown in the inset of Fig. 2B, the fluorescence decay kinetics recovered to the fast forward electron transfer and remained consistent up to 30 days, reflecting the standard pattern of electron transport from PSII.

Interestingly, even after 10 days of incubation in the batch culture, Chlamydomonas beads still maintained a F_V/F_M ratio of 0.35, approximately twice as high as that of free cells. After 30 days, the detected F_V/F_M ratio in beads still stood at around 0.32, indicating the retention of the PSII activity at approximately half of the initial level (Table 1). Remarkably, examination of the beads on this last day of incubation revealed a cell density of approximately 6 million cells per bead, exceeding the initial cell density by a factor of 5 (Table 2).

We also investigated the relative amount of PSII and PSI in the bead culture with EPR spectroscopy. Room temperature EPR spectra from the dark-adapted cells represent spectra from the oxidized Tyr_D ($Tyr_D^{\bullet}$ radical) residue in PSII and used as quantification of PSII. Spectra taken under illumination conditions, in addition, show oxidized $P700^+$ Chl radical and used as quantification of PSI [25,26,43]. The control beads on day 0 were dissolved, cells were concentrated as described in the methods section and EPR spectroscopy was performed (Fig. 3, black spectra). The PSI/PSII ratio, determined from this measurement was found to be 0.97, representing normal, almost equal amount of both photosystem present. Thus, the bead formation did not affect either the PSII, or PSI activity (Table 1). Interestingly, about 10 % of P700 was oxidized already in the dark in the control samples (Fig. 3, solid black spectrum).

3.3. DBMIB-induced H_2 production by immobilized Chlamydomonas cells

Recently, it was shown by us that the introduction of the inter-photosystem electron transfer inhibitor DBMIB at suboptimal

Table 2
Cell density in Chlamydomonas beads at the inception of formation and at the end of incubation in standard TAP medium and in the presence of DBMIB (3.5 μM). The results represent the average of three independent measurements.

Sample	Cell density (10^6 cells/bead)
Freshly formed beads	1.2
Beads from a 30-day batch culture (standard TAP)	6.0
Beads from 20-day batch culture (+3.5 μM DBMIB)	3.6

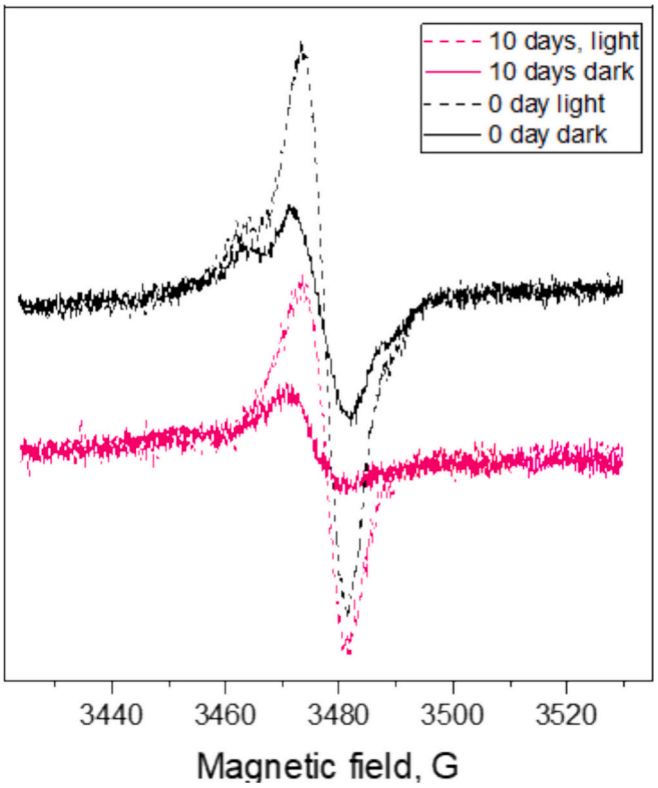


Fig. 3. EPR spectra from the dissolved fresh beads (black spectra) or after 10 days of incubation with 3.5 μM DBMIB (pink spectra). Spectra were recorded from the dark-adapted sample (solid line) or sample under illumination (dashed line). EPR conditions: microwave frequency 9.76 kHz, microwave power 8 mW, modulation amplitude 5 G, room temperature. (For interpretation of the references to colour in this figure legend, the reader is referred to the web version of this article.)

concentrations promotes H_2 photoproduction in the wild-type Chlamydomonas [26]. The introduction of the DBMIB inhibitor into the sealed media culture containing Chlamydomonas beads stimulated H_2 production across all studied concentrations of inhibitor (0–10 μM), without necessitating any further manipulations (Fig. 4A). The H_2 generation in the DBMIB-treated Chlamydomonas beads started to be quite visible on day 3 and persisted throughout the measurement period, with a total production of around 200 μmol H_2 per mg Chl within 20 days. The concentration of the DBMIB inhibitor had no substantial impact on the overall cumulative H_2 production, although a minor enhancement was noticeable at 3.5–5 μM concentration range, however, this difference lacked statistical significance. The peak rate of the H_2 production, reaching 33 μmol/mg Chl per day, was attained on day 6 after introducing 3.5 μM DBMIB, while the average H_2 production rate over 20 days using 3.5 μM DBMIB was roughly 10.6 μmol/mg Chl per day (Fig. 4A).

Surprisingly, wild-type Chlamydomonas cells immobilized in alginate beads exhibited promising levels of H_2 production even without any DBMIB addition. They initiated H_2 production from the first day of incubation at a small rate of approximately 0.5 μmol/mg Chl per day. This rate continued for the first two weeks of incubation, after which the H_2 production rate started to increase up to 10 μmol/mg Chl per day, terminating to a total amount of the produced H_2 of 77 μmol/mg Chl within 20 days. This outcome, although most likely a result of the fermentation process, is particularly interesting for further development since H_2 production was achieved in wild type cells, cultivated under standard growth conditions without any inhibitor.

For assessment of the PSII electron transport during H_2 production by Chlamydomonas beads, fluorescence decay kinetics were measured at

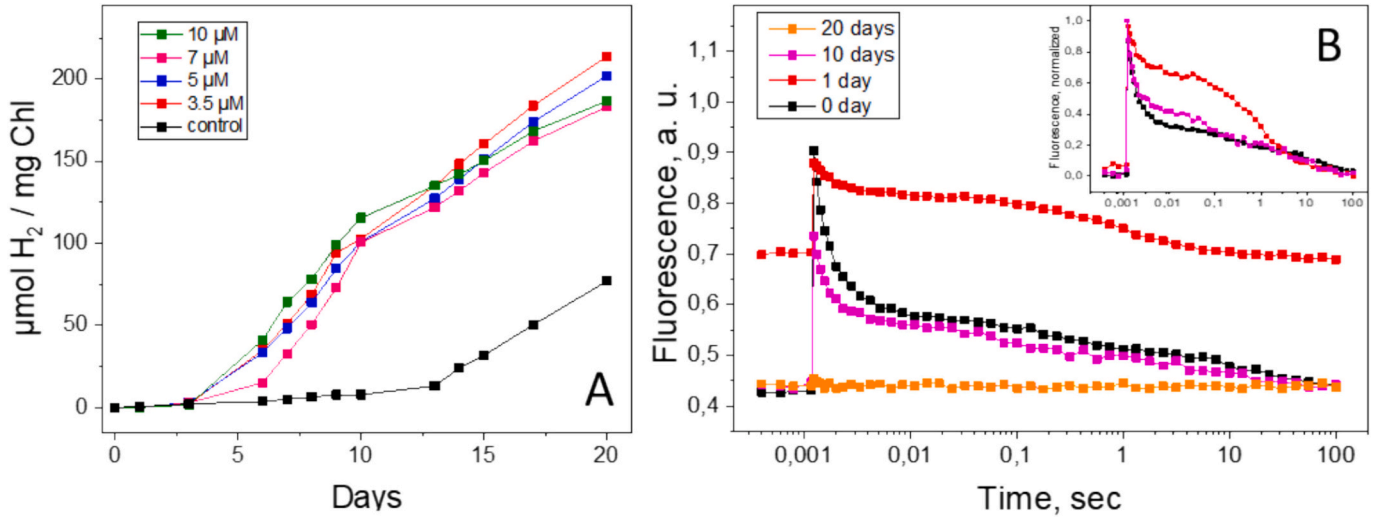


Fig. 4. A. Cumulative H_2 production by Chlamydomonas beads during 20 days of sealed batch culture incubation in TAP medium supplemented with different concentrations of DBMIB. B. Flash-induced fluorescence decay kinetics recorded in Chlamydomonas beads during 20 days of the batch culture incubation with TAP medium supplemented with 3.5 μM DBMIB inhibitor. The arrow marks the light flash application time and the inset shows normalized traces. Each trace in both graphs represents the average of measurements in three independent samples.

different time points following the addition of DBMIB. Two minutes after DBMIB addition, the decay kinetics did not reveal any significant difference from that of in the absence of DBMIB (Figs. 2B and 4B, black traces). However, the kinetics changed significantly after initial 24 h following the addition of DBMIB. As shown in Fig. 4B (red trace), F_0 increased from 0.4 to 0.7 without changing the F_M level (if compared to the black trace), and the decay kinetics became considerably slower (inset of Fig. 4B, red trace). This indicates a significantly slower forward electron transfer from PSII as result of the more reduced PQ pool, which aligns with the expected effect of the DBMIB presence.

Interestingly, the PSII electron transport characteristics recovered to a more normal state by day 10 of the experiment. The levels of F_0 and F_M, along with the decay kinetics, were very similar to those observed on day 0 (Fig. 4A, pink trace). However, after being in a batch culture for 20 days, the variable fluorescence almost completely disappeared (Fig. 4B, orange trace, Table 1). Unexpectedly, when beads obtained from day 20 were dissolved for subsequent cell counting, the result unveiled a cell density of 3.6 million cells per bead, surpassing the initial cell density in the fresh bead by threefold (Table 2).

EPR measurements on the beads after 10 days of the batch culture in the presence of DBMIB revealed a decreased amount of PSII corroborating our fluorescence data (Fig. 3, solid pink spectrum, Table 1). The amount of PSI was less affected, which resulted in almost twofold increase in the PSI/PSII ratio after 20 days of the H_2 production (Fig. 3, dashed pink spectrum, Table 1).

4. Discussion

4.1. Beneficial impact of immobilization on sustaining PSII activity

The improved cell viability within alginate beads is a well-established benefit of this immobilization technique [7–9,44–46]. However, the photosynthetic properties of immobilized Chlamydomonas cells have not been studied in great detail. Previous studies required dissolving alginate beads and separating the cells, subjecting them to significant stress and potentially disrupting photosynthetic reactions. In contrast, direct analysis of the intact beads offers more accurate insights into the photosynthetic status of entrapped cells. In this study we used fluorescence and EPR spectroscopy to assess photosynthetic properties during long-term incubation of Chlamydomonas alginate beads in vivo (Figs. 1B and 3). Comparative analysis of fluorescence decay changes during the long incubation period clearly demonstrated the superior capability of immobilized cells to maintain PSII activity over time. In free cells, after 10 days of incubation in the stationary phase, significant changes in fluorescence traces were evident, indicating a loss of the quantum efficiency of PSII and the slow forward electron transfer (Fig. 2A). In contrast, fluorescence traces obtained from beads illustrate a remarkably stable PSII activity even after 30 days of incubation (Fig. 2B). Only a minor over-reduction was observed during the initial 2 days of the cell entrapment within beads (Fig. 2B, inset), which could be attributed to an adaptation period of immobilized cells to the new environment, causing a transient over-reduction of the thylakoid membrane [47,48]. Subsequently, the conditions fully recovered and the electron transfer was maintained at the same optimal level as in the control cells for the remaining 28 days (Fig. 2B).

4.2. Characterization of H_2 production by DBMIB exposed Chlamydomonas beads

As anticipated, based on our previous investigative findings [24–26], the improved PSII stability in Chlamydomonas beads led to a significant increase in H_2 production by the DBMIB-treated beads if compared to the DBMIB-treated free cells (Table 3, Fig. 4A). Surprisingly, unlike in free cells [26], the H_2 production of DBMIB-treated beads did not exhibit concentration dependence above 3.5 μM. The reason for this is unclear, however, it might involve the diffusion limitation or stability of DBMIB in the alginate matrix.

Interestingly, the maximum rate of H_2 production by Chlamydomonas beads occurred on day 6 after the DBMIB addition, similar to what was observed in free cell culture with comparable values. This indicates

Table 3
A Comparison of H_2 production profiles between Chlamydomonas free cells and beads in the presence of 3.5 μM DBMIB over 20 days.

H_2 production properties	Free cells	Beads
Total produced H_2 in 20 days (μmol/mg Chl)	107	213
Average rate of H_2 production (μmol/mg Chl/day)	5.4	10.6
Max rate of H_2 production (μmol/mg Chl/day)	31	33
Min rate of H_2 production after first peak (μmol/mg Chl/day)	1.9	8.6

that metabolic processes leading to surge of H_2 evolution after partial inhibition of the inter-photosystem electron transfer is comparable in free and immobilized cells. These conditions prevailed for a long time since the average H_2 production rate over 20 days in beads was double of that in free cells, leading to a twofold increase in total H_2 production (Table 3). The more consistent profile of the extended H_2 production in beads stands out, highlighting the advantage of immobilization in maintaining the HydA activity and stability.

The analysis of PSII and PSI activities in the Chlamydomonas beads over the prolonged time period confirmed that sustaining photosynthetic reactions is likely contributed to the increased H_2 production. Although only half of PSII remained stable during the first 10 days as was shown by both fluorescence and EPR measurements (Table 1 and Fig. 3), it was remarkable that these PSII centers showed the same activity as in control cells (Fig. 4B) and continue to provide electrons for the HydA activity. Thus, the more preserved PSII activity translates into higher H_2 production by the DBMIB-treated beads. The role of PSI is also important. We observed increase in the PSI amount relative to PSII on day 10 of H_2 production by EPR (Fig. 3). We observed this trend before during long-term H_2 production in free cell cultures [25,26]. This is a probable response to a gradual elevation of the PQ-pool reduction level after DBMIB addition. However, the increase in the PSI amount we observed here was much less than in free cell cultures, which again points out the advantage of immobilization for maintaining not only PSII but also the PSI stability.

On day 20 after DBMIB introduction the evolved H_2 most probably originated from the indirect pathway. This assumption arises from the minimal PSII activity detected through fluorescence decay analysis on this day (Table 1, Fig. 4B). When the beads from this day were dissolved and examined under the microscope, 3.6 million cells per bead were observed, 3 times more than in the initially created beads (Table 2), all appearing healthy (data not shown). Therefore, even the minimal photosynthetic activity at high cell concentration was sufficient to maintain H_2 production in the immobilized Chlamydomonas cells.

In another scenario, the O_2 evolution activity of cells immobilized within the core of the beads may be impeded by the shading effect caused by peripheral cells. This shading effect, coupled with O_2 consumption through respiration, can induce hypoxic conditions for hydrogenase, thereby facilitating H_2 production via an indirect pathway involving PSI. This scenario can also elucidate how wild-type immobilized cells (without any treatment) could initiate H_2 production and demonstrate an elevated rate of H_2 production in the subsequent days of incubation. Enhanced photosynthetic stability within Chlamydomonas beads contributes to prolonged and increased H_2 production and reduces the need for cell and media culture replenishment, thereby lowering material and energy costs. This assumes greater significance when the future scaling up experiments will be considered.

5. Conclusion

In this study, we compared the photosynthetic electron transport properties between immobilized Chlamydomonas cells (encapsulated within alginate beads) and free cells using flash-induced variable fluorescence and EPR spectroscopy. Our findings emphasize the substantial advantage of immobilization in preserving PSII stability and activity, observed over an extended period of 30 days of incubation. This enhanced stability likely contributed to the sustained and increased H_2 production observed in immobilized cells treated with DBMIB. The combination of immobilization with the DBMIB treatment resulted in a two-fold increase in H_2 production, persisting for 20 days, with an average production rate double that of free cells.

These findings highlight the potential of immobilization techniques to improve H_2 production. However, it is essential to customize immobilization conditions and characteristics to suit each method of algal H_2 production. Further research in this direction could pave the way to the optimization and commercialization of algal H_2 production systems.

CRediT authorship contribution statement

Fatemeh Khosravitabar: Writing – original draft, Methodology, Investigation, Formal analysis, Data curation. **Fikret Mamedov:** Writing – original draft, Supervision, Project administration, Methodology, Data curation, Conceptualization.

Declaration of competing interest

The authors declare that they have no known competing financial interests or personal relationships that could have appeared to influence the work reported in this paper.

Data availability

No data was used for the research described in the article.

Acknowledgements

The authors wish to acknowledge the Carl Tryggers Foundation for Scientific Research for the financial support of the project (grant CTS 19:230). The first author was also supported by the Olle Engkvist Foundation (grant 218-0099) during the writing phase.

References

[1] C.-L. Soo, C.-A. Chen, O. Bojo, Y.-S. Hii, International Journal of Polymer Science (2017) 2017.
[2] M. Han, C. Zhang, F. Li, S.-H. Ho, Sci. Total Environ. 852 (2022) 158514.
[3] S. Vasilieva, E. Lobakova, A. Solovchenko, Environmental Biotechnology 3 (2021) 193–220.
[4] J. Pires, M. Alvim-Ferraz, F. Martins, M. Simões, Environ. Sci. Pollut. Res. 20 (2013) 5096–5105.
[5] M.K. Lam, K.T. Lee, Chem. Eng. J. 191 (2012) 263–268.
[6] F. Khosravitabar, J. Appl. Phycol. 32 (2020) 277–289.
[7] S.A. Covarrubias, L.E. de Bashan, M. Moreno, Y. Bashan, Appl. Microbiol. Biotechnol. 93 (2012) 2669–2680.
[8] S. Khan, M. Naushad, J. Iqbal, C. Bathula, G. Sharma, Fuel 311 (2022) 122543.
[9] C. Palito, T. Encarnação, P. Singh, A.J. Valente, A.A. Pais, Marine Microbial Bioremediation, CRC Press, 2021, pp. 122–141.
[10] S.P. Arimbrathodi, M.A. Javed, M.A. Hamouda, A. Aly Hassan, M.E. Ahmed, Water 15 (2023) 185.
[11] Y.M. Chen, Energ. Environ. Sci. 15 (2022) 2843–2857.
[12] G. Torzillo, A. Scoma, C. Faraloni, L. Giannelli, Crit. Rev. Biotechnol. 35 (2015) 485–496.
[13] L.Z. Wei, W.M. Ma, GCB Bioenergy 16 (2024) e13118.
[14] F. Khosravitabar, C. Spetea, Int. J. Hydrogen Energy 67 (2024) 925–932.
[15] J. Benemann, Int. J. Hydrogen Energy 22 (1997) 979–987.
[16] M.L. Ghirardi, R.K. Togasaki, M. Seibert, Appl. Biochem. Biotechnol. 63-65 (1997) 141–151.
[17] A. Scoma, D. Krawietz, C. Faraloni, L. Giannelli, T. Happe, G. Torzillo, J. Biotechnol. 157 (2012) 613–619.
[18] R. Surzycki, L. Cournac, G. Peltier, J.-D. Rochaix, Proc. Natl. Acad. Sci. 104 (2007) 17548–17553.
[19] M.G. Esquível, H.M. Amaro, T.S. Pinto, P.S. Fevereiro, F.X. Malcata, Trends Biotechnol. 29 (2011) 595–600.
[20] A. Melis, L. Zhang, M. Forestier, M.L. Ghirardi, M. Seibert, Plant Physiol. 122 (2000) 127–136.
[21] G. Philipps, T. Happe, A. Hemschemeier, Planta 235 (2012) 729–745.
[22] K.A. Batyrova, A.A. Tsygankov, S.N. Kosourov, Int. J. Hydrogen Energy 37 (2012) 8834–8839.
[23] A. Volgusheva, G. Kukarskikh, T. Krendeleva, A. Rubin, F. Mamedov, RSC Adv. 5 (2015) 5633–5637.
[24] A. Volgusheva, S. Styring, F. Mamedov, Proc. Natl. Acad. Sci. 110 (2013) 7223–7228.
[25] P.S. Krishna, S. Styring, F. Mamedov, Green Chem. 21 (2019) 4683–4690.
[26] F. Khosravitabar, F. Mamedov, Int. J. Hydrogen Energy 48 (2023) 36314–36326.
[27] T. Elman, T.T.H. Ho, Y. Milrad, M. Hippler, I. Yacoby, Cell Reports Physical Science (2022) 3.
[28] P. Liu, D.-M. Ye, M. Chen, J. Zhang, X.-H. Huang, L.-L. Shen, K.-K. Xia, X.-J. Xu, Y.-C. Xu, Y.-L. Guo, Photosynth. Res. 154 (2022) 397–411.
[29] F. Khosravitabar, M. Hippler, Int. J. Hydrogen Energy 44 (2019) 17835–17844.
[30] V. Nagy, A. Podmaniczki, A. Vidal-Meireles, R. Tengölics, L. Kovács, G. Rákhely, A. Scoma, S.Z. Tóth, Biotechnol. Biofuels 11 (2018) 1–16.
[31] J.M. Woon, K.S. Khoo, M. Akermi, M.M. Alanazi, J.W. Lim, Y.J. Chan, P.S. Goh, B. S. Chidi, M.K. Lam, J. Zaini, Fuel 346 (2023) 128312.

[32] T.K. Antal, T.E. Krendeleva, T.V. Laurinavichene, V.V. Makarova, M.L. Ghirardi, A. B. Rubin, A.A. Tsygankov, M. Seibert, Biochimica Et Biophysica Acta-Bioenergetics 1607 (2003) 153–160.
[33] S. Kosourov, H. Leino, G. Murukesan, F. Lynch, K. Sivonen, A.A. Tsygankov, E. M. Aro, Y. Allahverdiyeva, Appl. Environ. Microbiol. 80 (2014) 5807–5817.
[34] H. Leino, S.N. Kosourov, L. Saari, K. Sivonen, A.A. Tsygankov, E.M. Aro, Y. Allahverdiyeva, Int. J. Hydrogen Energy 37 (2012) 151–161.
[35] T. Sukrachan, A. Incharoensakdi, Journal of Applied Phycology 32 (2020) 1103–1115.
[36] T. Maswanna, P. Lindblad, C. Maneeruttanarungroj, Journal of Applied Phycology 32 (2020) 2937–2945.
[37] S.N. Kosourov, M. Seibert, Biotechnol. Bioeng. 102 (2009) 50–58.
[38] T.K. Antal, G.P. Kukarskikh, A.A. Volgusheva, T.E. Krendeleva, E. Tyystjärvi, A. B. Rubin, Algal Research 17 (2016) 38–45.
[39] S. Kosourov, G. Murukesan, M. Seibert, Y. Allahverdiyeva, Algal Res. 28 (2017) 253–263.
[40] A. Ruiz-Marin, L.G. Mendoza-Espinosa, T. Stephenson, Bioresour. Technol. 101 (2010) 58–64.
[41] S.M. Moreira, M. Moreira-Santos, L. Guilhermino, R. Ribeiro, Enzyme Microb. Technol. 38 (2006) 135–141.
[42] A. Volgusheva, O. Kruse, S. Styring, F. Mamedov, Algal Res. 18 (2016) 296–304.
[43] R. Danielsson, P.-Å. Albertsson, F. Mamedov, S. Styring, Biochimica et Biophysica Acta (BBA)-Bioenergetics 1608 (2004) 53–61.
[44] F. Santos-Rosa, F. Galván, J. Vega, J. Biotechnol. 9 (1989) 209–219.
[45] R. León, J. Pizzano, F. Galván, Progress in Biotechnology 11, Elsevier, 1996, pp. 221–228.
[46] M. Debowski, M. Krzemieniewski, M. Zielinski, J. Kazimierowicz, Atmosphere (2021) 12.
[47] J.-D. Rochaix, FEBS Lett. 529 (2002) 34–38.
[48] S. Mendez-Alvarez, U. Leisinger, R.I. Eggen, Int. Microbiol. 2 (1999) 15–22.